Research Article

Environmental Science and Climate Research

Meteorological Effects on the Performance of a Solid-State α-Detector Measuring Water Samples with Predefined Radon Concentration

Livhuwani Masevhe[1], Risimati Dazmen Mavunda[1]* and Simon Connell[1]

1University of Johannesburg (UJ), South Africa

*Corresponding Author
Risimati Dazmen Mavunda, University of Johannesburg (UJ), South Africa.

Submitted: 2023, Oct 12; **Accepted:** 2023, Nov 08; **Published:** 2023, Nov 13

Citation: Masevhe, L., Mavunda, R. D., Connell, S. (2023). Meteorological Effects on the Performance of a Solid-State α-Detector Measuring Water Samples with Predefined Radon Concentration. *Env Sci Climate Res, 1*(1), 33-45.

Abstract

The current study validates an α-spectrometry method by assessing the functionality and response of a solid-state alpha detector to known Radon concentrations, outdoor weather conditions and varied sample volumes. These all have an influence on the sample's behaviour inside the detector. Five samples of water with known radon concentrations (ranged from 90.66±7.20 mBq.l^{-1} to 314.65±24.6 mBq.l^{-1}) were used. The experimental setup used a radon-stripping unit connected to a continuous radon monitor, which measured the 222Rn in the water by counting α-particles emitted by its progeny in secular equilibrium. The effects of meteorological parameters such as the sample concentrations and volume, internal temperature and relative humidity inside the detector were observed. The analysis of the fluctuations of temperature and relative humidity in the detection chamber were found to be in agreement with theoretical predictions and outcomes of other previous studies. To calibrate the detector of choice, the same standard samples were measured by a liquid scintillation counter (LSC) which was considered as a reference detector in the current study. The two techniques gave similar trends in the results. The LSC results appeared to be consistently lower than those of the α-spectrometry as seen by the RAD-7 device. The α-spectrometry system based on a solid-state detector had a good resolution of the peaks (FWHM of 18.61 keV and 20.93 keV) which was better than that of LSC (FWHM 166 keV) whose peaks could not be resolved. The energy-tailing of the LCS spectrum caused by Compton Scattering led to a higher count-rate of 4.11 cpm for the LSC compared to 0.71 cpm for the RAD-7. The study demonstrated that α-spectrometry method as deployed in the RAD-7 device is the most suitable equipment for the measurement of radon concentration in water because of its superior sensitivity.

Keywords: α-Spectrometry, Standard Sample, LSC, Radon.

1. Detection and Measurement of Radon in Water

In the current study, the radon (^{222}Rn) concentration in water was measured using the α-spectrometry technique. ^{222}Rn is a naturally occurring colourless, odourless, and invisible radioactive gas resulting from the decay of ^{226}Ra in the uranium-series decay chain. It is commonly transported freely via faults and fragmented rocks and soils to the open atmosphere, surface dwellings, underground water and cavities [1]. Exposure to radon is considered the second leading cause of lung cancer after smoking [2]. Because of the damage it causes when inhaled or ingested in human body, it is always important to make precise measurements of radon in the environment. A number of detectors have been developed to fulfil this task, such as low-level proportional counters, Liquid Scintillation Counters (LSC), Lucas cell scintillation chambers, cryogenic detectors, and electrostatic chambers and finally by α-spectrometry with high-resolution solid-state detectors [3-7]. For the proper functionality of the equipment, the effect of meteorological parameters should be taken into consideration and be tested. Because radon is an inert gas, it dissolves in water, but does not react with water. Radon-in-water can either be measured in the laboratory after collecting the samples, taking into account the decay correction or measured in-the-field [8].

The aim of this study is to assess the performance and functionality of a specific radon detector under different conditions which are influential to the release of radon. The detector-of-choice was the solid-state alpha detector system, the RAD-7 radon detector. The RAD-7 radon detector was deployed in this research at the Necsa Radiation Protection Training Centre, although the calibration system described here could be used with other types of radon monitoring equipment. Measurement of radon concentration on a standard sample prepared in the laboratory with a known concentration was carried out by counting α-particles emitted by the progeny of radon, ^{218}Po and ^{214}Po [9]. In order to determine if the detector is working properly, it has to be calibrated by using standard samples with known radon concentration. Secondly, for

a control process of this experiment, the LSC detector was used to measure radon concentration from the same standard sample and compare with that measured with RAD-7 detector.

2 The Detector of Choice

2.1 Alpha-spectrometry using Solid-state Alpha Detectors

Alpha spectrometry is a widely applied radio-analytical technique, primarily due to its high counting efficiency, good energy resolution, low intrinsic background, its versatility in terms of both the range of radionuclide and sample types which can be analyzed and the reliability of the technique due to the possibility to use an a α-emitting isotope of the element of interest as an internal tracer [10].

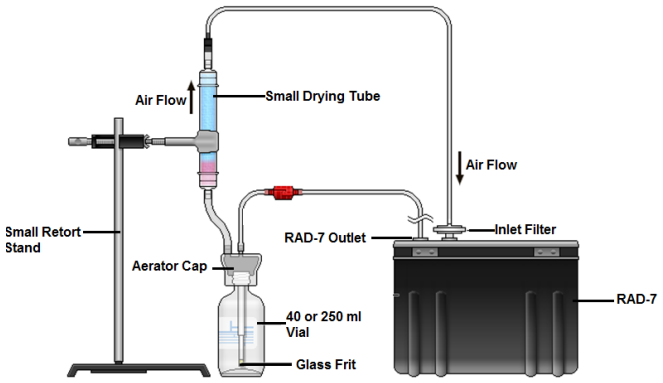

Figure 1: Schematic representation of the experimental setup using a grab sample and a radon-in-air monitor, a α-spectrometry method [11].

Figure 1 represents an experimental set-up using a grab sample and a radon-in- air monitor, which uses well defined signals in a solid-state alpha detector as a continuous radon monitor. The monitor applies the α-spectrometry process. It is a highly versatile instrument, used to measure radon in real-time and designed to detect α-particles only [12, 13]. The detector's major advantage is its high sensitivity, with detection limits as low as 1 mBq per sample being easily achievable.

The interior of the RAD-7 instrument contains a hemisphere of 0.7 l volume with an ion-implanted silicon solid-state α-detector, and an air pump to be found at the centre. A representation of the measurement chamber with the detector is shown in Figure 2 [14]. The high voltage power circuit charges the inside conductor to a potential of 2 000 to 2 500 V, creating an electric field throughout the volume of the detector [15]. The radon in the air is sucked inside and it decays into the positive ions of $^{218}Po^{+}$ ($T_{1/2}$ = 3.05 min; α-energy = 6.00 MeV) and $^{214}Po^{+}$ ($T_{1/2}$ = 164 ms; α-energy = 7.67 MeV), which are attracted by the electric field and may be deposited on to the detector, which is at ground potential, before they are neutralized [16]. The emitted α-particles of characteristic energy produce an electrical signal pulse. This set-up avoids the energy broadening effect due to alpha particle energy loss in different air layer thicknesses, as all alpha decays will happen on the detector surface. As such, especially high-resolution spectra are obtained.

The signal is amplified electronically and transformed into a digital signal and the energy of the signal is histogrammed by the microprocessor to form a spectrum [17]. The energy of the α-particle is linearly proportional to the electrical pulse voltage [17]. One of the many advantages of using this detector is its ability to immediately differentiate between different radionuclides by their α-energy using a α-spectroscopy (e.g. separate radon from thoron by the energy) [18]. The humidity inside the chamber must be kept low to prevent the ions from being neutralized so that the positive ion collection efficiency is high [18]. This explains the need for the desiccant, a laboratory-drying unit that is made of CaSO4 granules, which have a high affinity for water, so it absorbs moisture before it reaches the RAD-7 detector chamber [18]. Normally the RAD-7 instrument operates well at a humidity of less than 10 % and activity can be measured below 4 $Bq.m^{-3}$. The RAD-7 radon detector is a high-performance instrument which can determine the activity of ^{222}Rn continuously by electrostatic collection and measurement of the alpha-emitting daughters, ^{218}Po and ^{214}Po [19, 11].

2.2 The Reference Detector

For the purpose of establishing a control measurement for the detector of choice, it is quite important to analyze its efficiency against a control detector and establish if α-particle spectrometry in the RAD-7 detector is the most appropriate for radon progeny measurements. The Liquid Scintillation Counter (LSC) housed at Necsa's Radio-Analysis Laboratories was employed for the current study as reference detector. The set-up in Figure 2 schematically presents the main components and their functions within an LS counter.

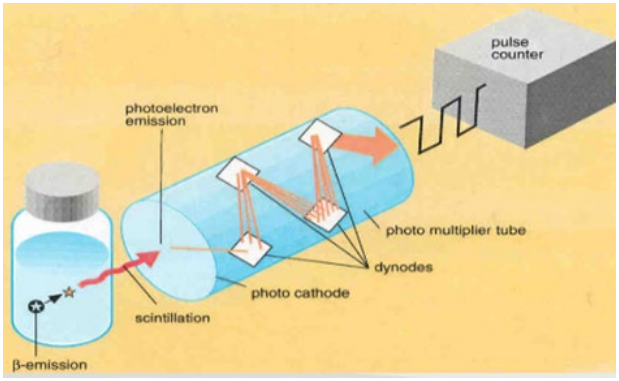

Figure 2: schematic representation of liquid scintillation counter operation principle [20].

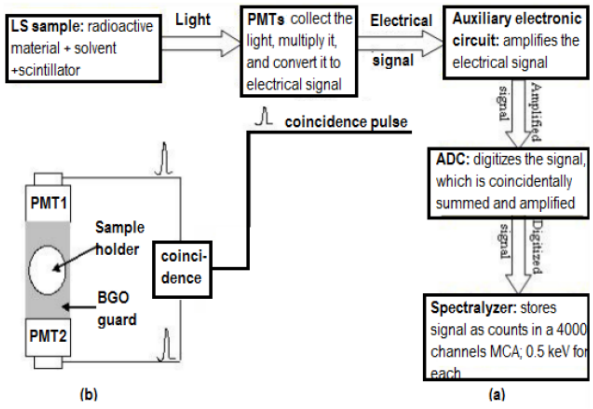

Figure 3: Illustration of LSC principle. (a) Flow chart summarizing the main components of a Liquid Scintillation Counter, their respective functions and outputs. (b) Schematic diagram of a detection section of a Packard TRI-LSC system [21].

Figure 2 is a flow chart illustrating a water sample mixed with a cocktail, consisting of a scintillator and a solvent. The radiation emitted in the decay of radon and its progeny causes excitation of the scintillator molecules, which subsequently de-excite by emitting light. The emitted light is collected by photomultiplier tubes (PMTs) and converted into electrical pulses that are amplified by auxiliary electronics. The intensity of the scintillation light is linearly proportional to the deposited alpha energy [22, 23].

The signal is processed (digitized and histogrammed) and displayed as a spectrum on a 4 096 channel multi-channel analyzer (MCA). The calibration is set so that each channel corresponds to an energy of 0.5 keV. In LS cocktails, the kinetic energy of an α-particle is scaled by a factor of about 10 due to the fact that α-particles produce pulses of longer duration in the LS cocktail compared to β-pulses, e.g. alpha energy of 6.0 MeV appears at 600 keV. The consequence is that in the LSC, the α-spectrum overlaps with the high-energy β-spectrum. Hence, LSCs usually incorporate a pulse-shape discrimination mechanism to distinguish between pulses from alphas and of high-energy betas [22].

2.3 Quality Control for α-Spectrometers

The performance of the RAD-7 instrument was verified by counting the sample from the same source in the LSC [24]. The same standard sample containing at least two α-emitting radionuclides, which are ^{218}Po and ^{214}Po, was used to check their energies, the Full Width Half Maximum (FWHM) and the efficiency calibration of the detector or α-spectrometer [24]. The sample was measured in both techniques under similar conditions discussed below. The parameters characterizing the stability of the system are the peak location, the FWHM, and the counting efficiency of a selected radionuclide present in the standard source [24].

3. Methodology

3.1 Sampling Techniques

3.1.1 Standard Sample Preparation

Preparation and measurement of radon aqueous standard solutions are applicable to the continuous radon monitor (CRM) and LSC methods. The standard solution was prepared for both methods and it was used for the analysis to verify the results of the analysis from α-spectrometry CRM using LSC. For quality assurance (QA) regarding this approach, the aqueous standard solutions of different ^{226}Ra activity concentrations were prepared using a reference ^{226}Ra standard solution ACS/DC48/01 of 2003. The initial ^{226}Ra standard activity was used to prepare the master solutions of 2.07 ± 0.07 kBq.g^{-1}. Figure 4 shows the standard samples prepared in

the laboratory. Two sets of five known different Radium activity concentrations which were placed in closed vials and kept for 30 days to allow the decay equilibrium between ^{226}Ra ($T_{1/2}$= 1600a), its immediate daughter ^{222}Rn and the four short-lived radon progenies. The presence of ^{210}Pb and its progeny was neglected due to the long half-life of ^{210}Pb ($T_{1/2}$ = 22:3a) [9].

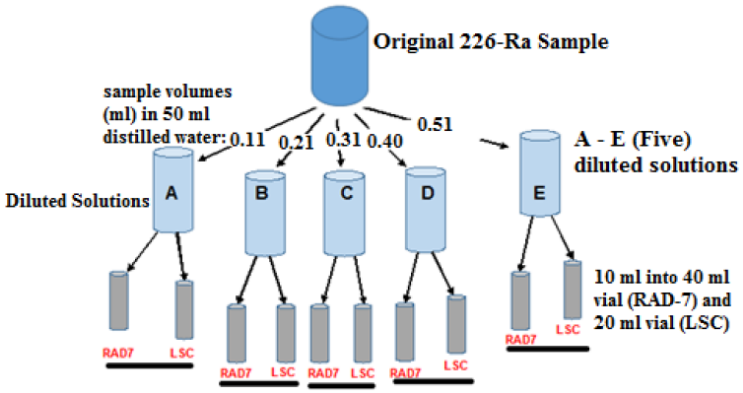

Figure 4: Laboratory prepared 226Ra standard samples prepared from Necsa's Radio-analysis Laboratory [9].

The Radon concentration in the water-filled volume of the sample-holder, is measured by the RAD-7 detector as shown in the experimental set-up in Figure 5. This system of equations can easily be solved for the radon concentration measured in the air-filled volume of the sample-holder and displayed by RAD-7, C, which is expressed as a function of the thickness of the sample (or sample height):

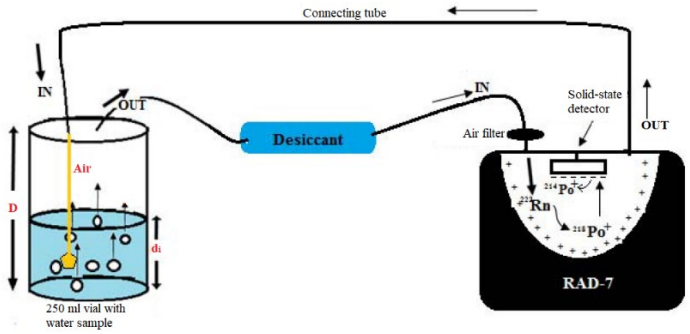

Figure 5: Schematic diagram of the system using a grab sample and radon-in-air monitor, RAD-7 [9].

3. 2 RAD-7 Calibration

The main purpose of this exercise was to study the effects of meteorological parameters on the performance of the detector. The standard samples with predefined radon concentrations were analysed under the following parameters, variation sample concentrations and volumes, and the effects of RH and internal temperature [9].

3.2.1 Sample Concentration

The detector was calibrated with 222Rn standards prepared (see Figure 4) with different concentrations 92.06, 178.46, 262.59 and 336.97 mBq.l-1. The correctness of the results would be established by comparing the measured radon concentration in the samples against the standard sample concentrations. The results were also compared with LSC radon detector measurements.

3.2.2 Sample Size

The discrete sample volumes of 1, 2, 3, 4 and 5 ml were extracted from the standard solution and were overlaid with distilled water to fill up the vial to determine the effects of sample volumes on the radon concentration. The relationship between the dilution factor and the radon content in the samples was also studied. Verification of the sample volume effects was also done using the LSC detector.

3.2.3 Sample Temperature

Five series of individual experimental runs, each performed at a different temperature to determine the effects of sample temperature on the release-rate of radon from the sample. Sample vials were submerged in a water bath to control the temperature during the radon degassing for all five different temperatures [144]. Setups were carried out with the sample's temperatures at 4, 9, 14, 19 and 24°C. To achieve 4°C, the sample vial was submerged in ice water in the bath whilst the 24°C temperature was reached by warming the water in the bath.

3.2.4 Sample Height in the Vial

In this section, a formula is derived to calculate the radon concentration (C) in the water-filled volume of the sample-holder, measured by the RAD-7 detector as shown in the experimental set-up in Figure 4. The radon concentration in the water will depend on the elevation coordinate, z and diffuse as described by the steady-state transport equation [25]

$$\frac{d^2C(z)}{dz^2} - \frac{\lambda\beta C(z)}{D} + \frac{G}{D} = 0, \quad (1)$$

where D is the radon diffusion coefficient in the water, λ is the radon decay constant and β=(1-m+Lm)$\underline{\varepsilon}$ is the partition corrected porosity taking into account porosity (ε), water saturation (m) and the partition coefficient of radon between water and air phase (L). On the bottom of the sample-holder, $dC(z)/dz|_{z=0} = 0$. The boundary condition on the top surface of the water sample states that the activity concentration of radon in the water equals that in the air-filled volume of the sample-holder, $C(z=h)=C$.

The rate of change of radon activity concentration in the air-filled volume of the sample-holder is described by the following differential equations, which however, under steady-state conditions, reduces to an algebraic equation [25]:

$$\frac{dC(t)}{dt} = J\frac{1}{H-h} - \lambda C - \frac{q}{V}C + \frac{q}{2V}C = 0, \quad (2)$$

The resultant radon exhalation rate at the water-air interface can be then determined by

$$J = -D\varepsilon\left(\frac{dC}{dz}\right), \quad (3)$$

where $dC(z)=dz$ is determined as the solution from Equation 2, using the appropriate boundary conditions, Equation 3 becomes

$$J = E \times e^{\rho Ra\lambda L} \times \tanh\left(\frac{H}{L}\right), \quad (4)$$

where H is sample thickness and L is diffusion length with $L=qDL$. This system of equations can easily be solved for the radon concentration measured in the air-filled volume of the sample-holder and displayed by RAD-7, C, which is expressed as a function of the thickness of the sample (or sample height) [25]:

$$C(h) = \frac{G\lambda \times \tanh(k_w h)}{\beta + k_w(2\lambda(H-h)A + q)} \quad (5)$$

where, $k_w = \sqrt{\lambda\beta/D_w}$.

4. Results

4.1 Calibration

4.1.1 Inter-comparison between RAD-7 Instrument and LSC

The validation of the functionality of the detector of choice in the current study, simultaneous measurement using standard samples of radon concentration was carried out to get an inter-comparison between the RAD-7 and LSC instruments. The measured values of radon concentration from the two instruments presented in Table 1. The measured concentrations varied from 90.7±7 mBq.l^{-1} to 314.7±25 mBq. l^{-1} and 40.3±28 mBq. l^{-1} to 255.5 ± 11 mBq. l^{-1} for the α-spectrometry technique and the LSC, respectively.

Vial	Rn-C_{Std} (mBq.l^{-1})	Rn-C_{RAD-7} (mBq.l^{-1})	Rn-C_{LSC} (mBq.l^{-1})
A	92.1	91 ± 7	40 ± 28
B	178.5	136 ±19	83 ± 20
C	262.6	242 ± 27	149 ± 15
D	337.0	315 ± 19	255 ± 11

Table 1: Radon standard sample concentrations measured by RAD-7 and LSC detectors.

Parameters per Detectors	RAD-7 Detector	LSC Detector
Peak position (MeV)	6.05 (^{218}Po)	7.51 (^{218}Po)
	7.90 (^{214}Po)	8.31 (^{214}Po)
Resolution (FWHM) (keV)	18.61 (^{218}Po)	166
		20.93 (^{214}Po)
Counting efficiency (%)	90.03	50.6

Table 2: The parameters characterizing the stability of the system.

Observations showed that α-spectrometry technique closely matched with that the standard sample by a factor pf 0.9 while the LSC factor was 0.6. It is clear from the measurements that the α-spectrometry in the RAD-7 instrument to be more reliable in comparison with other radon monitors. Therefore, the RAD-7 instrument can be used in low and high radon environment, it is portable and can be useful for a general survey even in the dwellings or fields.

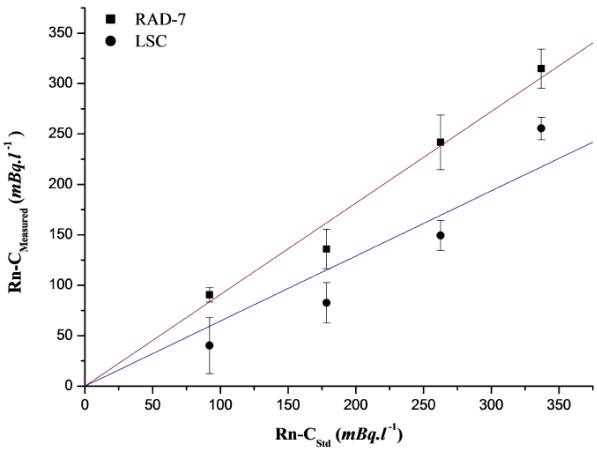

Figure 6: Measured radon concentration by two methods the RAD-7 and LSC the as a function of the standard concentration.

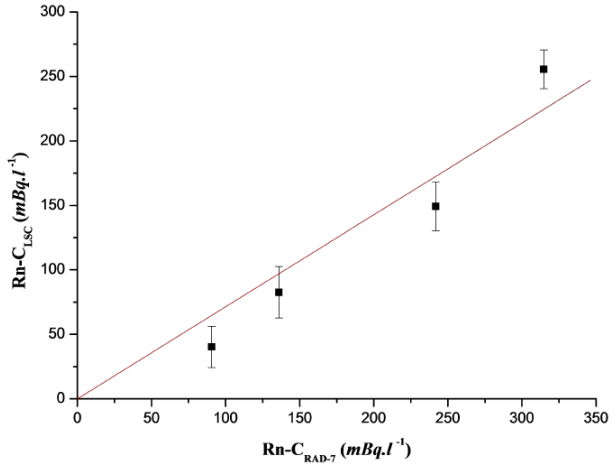

Figure 7: Correlation between the RAD-7 and the LSC detectors.

4.1.2 Spectra Analysis

When charged, ^{218}Po and ^{214}Po ions impact onto the surface of the detector in the internal cell of the RAD-7 instrument, this produces a signal which when accumulated and stored, resulted in a spectrum with an energy scale from the calibration (Figure 8). The spectrum scale divided into 200 channels (of 0.05 MeV each) and selected regions grouped into 8 energy windows of which the four major ones were A, B, C and D. The two peaks with resolutions (FWHM) 19 keV (^{218}Po) and 21 keV (^{214}Po) shifted to the right by 50 keV and 210 keV, respectively.

Figure 8 presents the energy spectrum of ^{222}Rn and its progeny for the same standard sample of 92.06 mBq.l-1, measured with the LSC instrument with three peaks of ^{222}Rn, ^{218}Po and ^{214}Po with the energy shifted to the right by almost 2 MeV. The cause of the shift of the peaks was due to energy loss in the transfer from solvent to solute or the attenuation of light photons in the solution. The scintillometer efficiency factor (1.86) obtained here was over the range 0 – 10 240 keV energy window [113], chosen for the refined α/β-separation capability and lower background. The spectrum was characterized by a relatively poor resolution with a FWHM of 166 keV and the variation of the resolution as a function of energy is more than in semiconductor α-spectrometry [113].

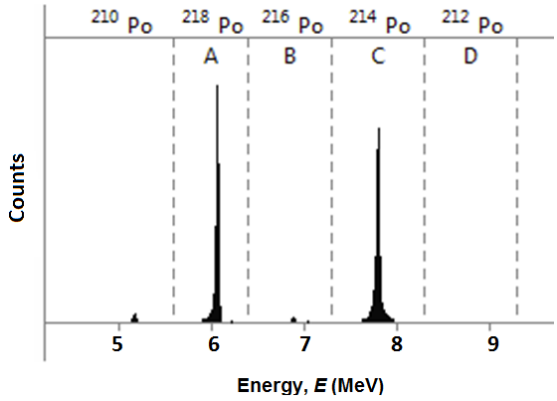

Figure 8: Spectroscopy of the standard sample (92.06 mBq.l^{-1}). RAD-7 instrument alpha spectrum showing peaks of ^{218}Po and ^{214}Po.

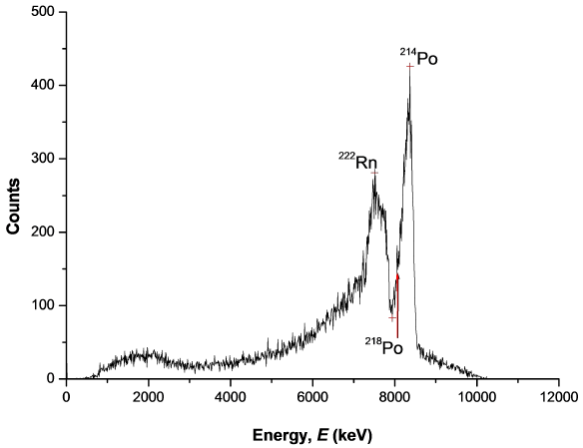

Figure 9: Energy spectrum obtained for determining ^{222}Rn, ^{218}Po and ^{214}Po activity and concentration.

This resolution does not allow the detection of the individual alpha lines belonging to the various α-emitting isotopes. In Figure 9 the α-radiation of 218Po and 214Po appears in a single common peak and cannot be resolved [113]. The energy-tailing was caused by Compton Scattering. The summary of QCs between RAD-7 and LSC in this study are presented in Table 4.2. This discussion further emphasizes the preference of selecting the RAD-7 instrument for radon concentration determination over the LSC instrument, and it lends additional credibility to the results that will be obtained, as the survey instrument is more reliable. Therefore, the method of α-spectrometry technique as embodied in the RAD-7 instrument was an appropriate choice as it is more precise and less susceptible to interferences than other instruments, for the task in hand.

4.2 Effects of Varying Sample Geometry Parameters on the Radon Concentration

4.2.1 Effects of Sample Volume

The experimental results of the effect of five different volumes of the water sample that was collected from the Hartbeespruit River, *Vs* (1, 2, 3, 4 to 5 ml) on the radon concentration in the sample. The results show that when the sample volume increased, the radon concentration slightly increased. Figure 10 the radon concentration as a function of the sample volume. The radon concentration increased by a factor of 4 between the first sample volume which was 1 ml to the last volume of 5 ml. Ideally, the concentration was supposed to remain the same because all five volumes were taken from the same sample. Since the basic volume of the air chamber in the RAD-7 instrument, desiccant and tubes are fixed, any variation of air volume is dependent on *Vs* in the vial [1].

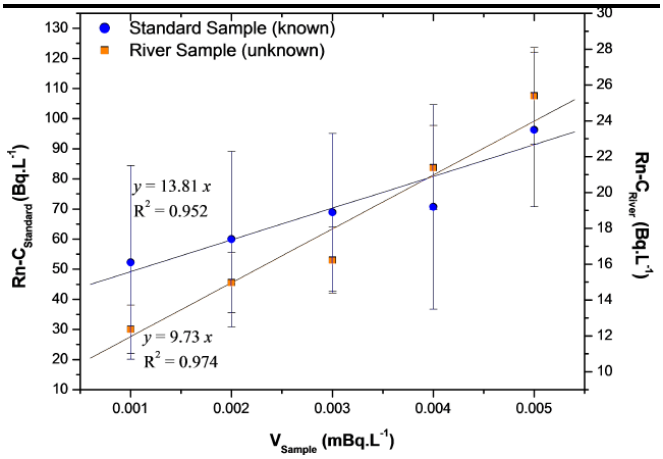

Figure 10: Radon concentration measured by RAD-7 as a function of the standard sample and river sample, and Correlation between RAD-7 and LSC at different sample volumes.

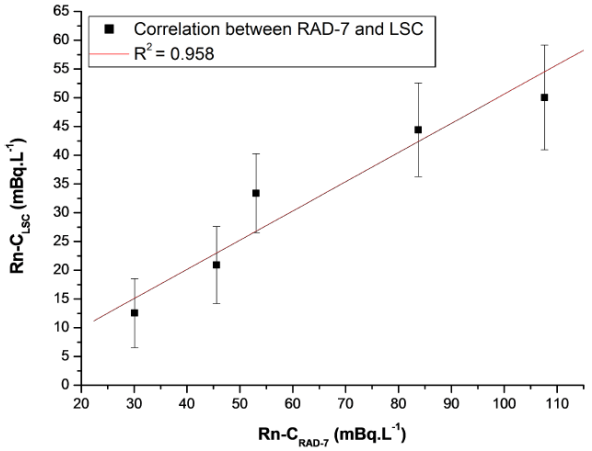

Figure 11: Correlation between the RAD-7 and the LSC techniques applied for measurements of 222Rn in different Vs in the range from 0.001- 0.005 L.

The experimental results indicated that the volume of water sample, Vs had a little effect and can be useful in the determination of radon concentration in water. Therefore, a bigger volume of the sample is recommended for future studies.

4.2.2 Effects of Internal Temperature and Relative Humidity

A radon concentration was detected in the water samples from the Walkerspruit River with an average radon concentration of 35 mBq.l^{-1} using RAD-7 instrument at different relative humidity (RH) and internal temperature (T_{int}) values, as shown in Table 3. The effects of increased RH and Tint from 14 % to 24 % and 21℃ to 22 ℃ respectively have an impact of the functionality of the detector in terms of its counting efficiency. It was observed that the radon concentration varied from 34.2 ± 8 mBq.l^{-1} to 26.6 ± 1.5 mBq.l^{-1} while the relative humidity and temperature inside the RAD-7 instrument varied. The average radon concentration measured in this sample was 31.2 ± 7 mBq.l^{-1}.

Measurement time (min)	T_{int} (℃)	RH (%)	Rn-C (mBq.l^{-1})
5.00	20.55 ± 1.82	13.09 ± 1.82	34.22 ± 8.14
13.00	20.98 ± 0.21	17.64 ± 1.13	33.79 ± 9.41
21.00	21.45 ± 0.16	20.50 ± 0.50	31.49 ± 7.40
32.00	22.01 ± 0.28	22.36 ± 0.51	29.72 ± 7.16
36.00	22.35 ± 0.17	24.00 ± 0.50	26.60 ± 1.50

Table 3: The effect of relative humidity and internal temperature on the response of the RAD-7 during the measurement period.

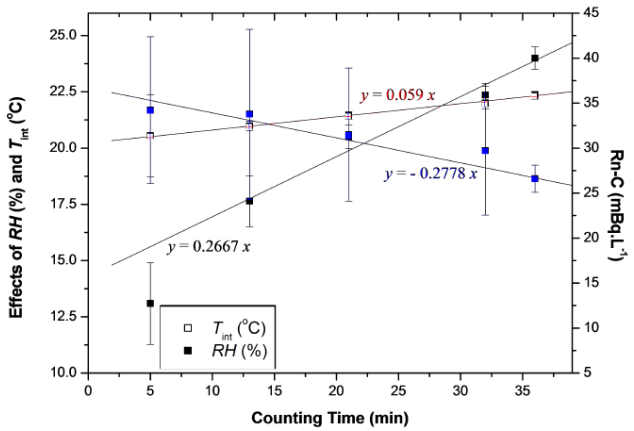

Figure 12: The effect of changes in the relative humidity, internal temperature on the radon concentration during the counting period inside the RAD-7 detector using the Walkerspruit water sample.

The internal temperature (T_{int}) and bias voltage affect the measurement of radon concentration when using the RAD-7 instrument. The performance and characteristics of the electrostatic collection rate of ^{222}Rn by the detectors are dependent on the charge of the uranium progeny atoms. In the RAD-7 detector, a high electric field of 2 keV in the detection chamber propels the positively charged ^{218}Po and ^{214}Po, onto the detector (Figure 12) [26]. The movement can be hindered by an increase in relative humidity, RH, inside the detection chamber. According to Batta (Radon in the DRIFT-II, 2015)," Being a polar molecule, water vapour attracts ions and hence reduces the instrument's sensitivity by preventing radon daughters from reaching the sensitive part of the detector [27]. As the RH rises, radon concentration decreases, Figure 12. A similar reasoning based on the survival of ions in their charged state would apply for the internal temperature variable" [27].

The effect of the relative humidity on the measurement was caused mainly from the continuous circulation of incoming air to the detection chamber of the RAD-7 instrument [27]. Figure 12 showed that when *RH* and T_{int} increase in the internal cell of the detector, less radon concentrations were counted by the detector [27]. The inverse relationship between *DRH* and D_{Tint}, and the radon concentration measured by the detector is presented in both figures. The results in Table 3 proved that *RH* has an influence over radon detection. Figure 4.8a further shows that the highest radon concentration occurs at the lowest *RH* percentage.

4.2.3 Sample Temperature

Table 4 and Figure 13 showed the influence of the change in sample temperature (T_{sample}) to the release of radon concentration from the sample. When the T_{int} increased, more radon concentration was released from the sample into the detector which resulted in more concentration counted as presented in Table 4. Radon solubility decreases with increase temperature (see Figure 13(b)). An increase of sample temperature increases the release rate from the water as shown in Figure

T_{sample} (°C)	C_{water} ($Bq.l^{-1}$)	R_{rate}
4.00	93.21 ± 3.62	1.55 ± 0.06
9.00	123.97 ± 10.13	2.07 ± 0.17
14.00	130.10 ± 7.09	2.17 ± 0.12
19.00	154.97 ± 12.31	2.58 ± 0.21
24.00	169.32 ± 6.99	2.82 ± 0.12

Table 4: The effects of sample temperature (T_{sample}) on radon concentration release rate and its partition coefficient in water samples. Experimental setup of sample volume (V_s) and total air volume (V_a) in the system, V_a of 0.25 L and 1.34 L, respectively

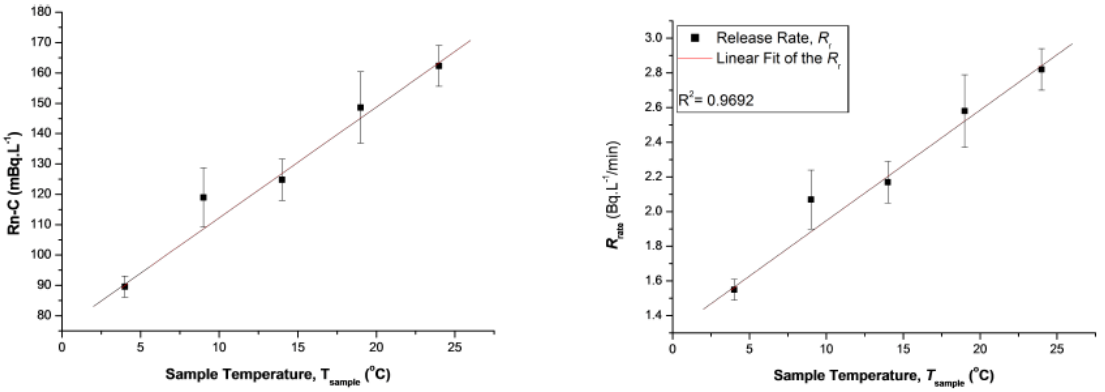

(a) Effects of T_{sample} on radon concentration

(b) T_{sample} – Release-rate correlation

Figure 13: Effects of the change of sample temperature on the release of radon concentration in the water.

4.2.4 Sample Height

Table 5 showed the effects of sample height, *h*, (Column 2) on radon concentration using RAD-7 detector. The height of the sample was increased in the interval of 0.01 m resulted in a non-linear increase of radon concentration (see Column 3). Radon concentration of the samples that was collected from the river in the vial increases from 0.72 ± 0.22 $mBq.l^{-1}$ – 2.13 ± 0.38 $mBq.l^{-1}$.

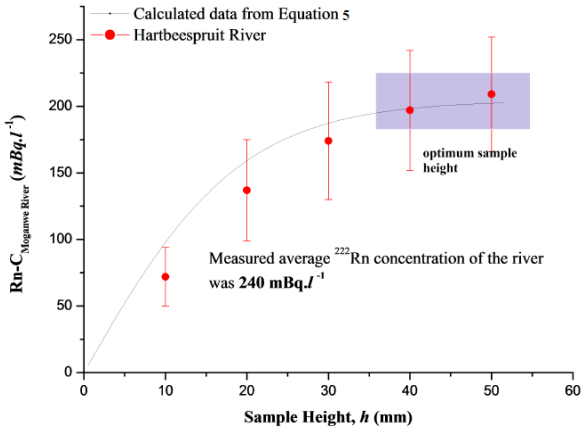

Figure 14: Radon concentration as a function of sample height, h in the sample-holder [9].

Vial No.	h (m)	*Moganwe$_{RAD-7}$ (mBq.l^{-1})	C$_{Theory}$ (mBq.l^{-1})
A	0.01	72 ± 22	97.73
B	0.02	137 ± 38	159.15
C	0.03	174 ± 44	187.29
D	0.04	194 ± 45	198.30
E	0.05	209 ± 43	202.35
F	0.06	213 ± 38	203.80

Table 5: The relationship between the sample height, h in the sample-holder using the RAD-7. The sample was collected from Moganwe River, Pretoria West [9].

The radon concentration measurement at different values of h, is graphically presented on Figure 14 together with the curve of the best fit of the model formula. The mathematical model of the measurement technique described well the response of RAD-7 as a function of h.

4.3 Time-Series

Since the RAD-7 is a counting system in a closed air-loop, only decay and leakage would lead to lower concentrations over time. The plotted data in Figures 15(a) and (b) shows that there were reduction of radon activity concentration during the counting periods which were about 85 hours (3.5 days) and 3 hours, respectively [9]. The theoretical loss was calculated by use of the radioactive decay equation,

$$A = A_0 e^{-\lambda t} \quad (6)$$

where A0 is the initial radon concentration; At observed concentration at time, t and l is radon decay constant (0.00755 h-1).

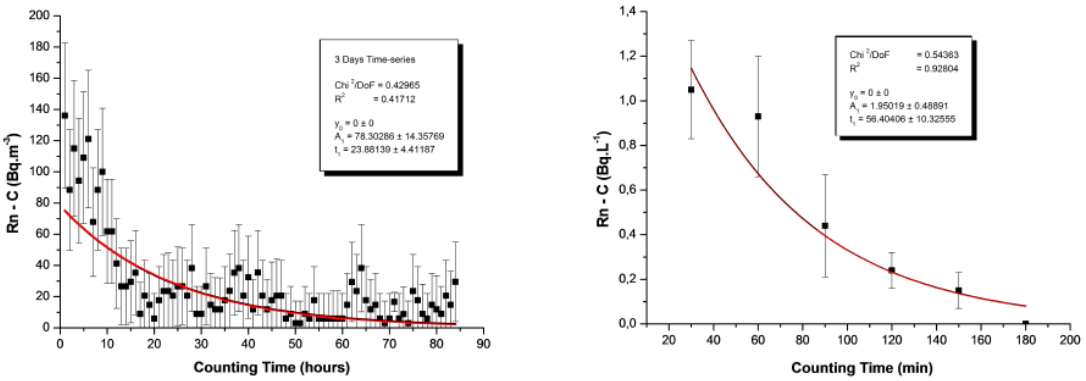

(a) 85 hours of counting time. **(b)** 3 hours of counting time.

Figure 15: Radon concentration decays in the RAD-7 internal cell over time.

5. Conclusion

In the current study the RAD-7 detector at the RPTC at Necsa was calibrated by assessing different conditions under which the detector is operated in the local environment. The detection system was calibrated and cross-checked against the LSC. The calibration coefficient between the RAD-7 and LSC is shown in Figure 7 (y = 0.713x) with the correlation coefficient of R2 = 0.91 and reduced chi-square of the fit of 0.81 [96]. The RAD-7 (detector of choice) was operating satisfactorily with a confidence level of 99.5%. The RAD-7 shows a much better resolution (FWHM 16.2 keV) than LSC (FWHM 166 keV). The RAD-7 was found to be a reliable and high-sensitive detector for radon determination in the water. An increase in sample temperature (Tsample), sample volume (Vsample) and sample thickness (h) showed an increased radon concentration which is directly related to radon release-rate from soil or rocks. The performance and characteristics of electrostatic collection rate of 222Rn by the detectors are dependence on the charge of the uranium progeny atoms. In the RAD-7 detector, a high electric field of 2 keV in the detection chamber propels the positively charged 218Po and 214Po, onto the detector (Figure 6).

The movement can be hindered by an increase in RH inside the detection chamber. Being a polar molecule, water vapour attracts ions and hence reduces the instrument's sensitivity by preventing radon daughters from reaching the sensitive part of the detector. As the RH rises, radon concentration decreases, Figure 12. Electronic noise generate energy in the form of heat inside the detector which caused an increase in internal temperature (T_int) resulting in peak tail as shown in the energy spectrum, Figure 12 [28]. An increase in Tint inside the detector compromised its counting efficiency. The results showed that the system provided very reasonable calibration results with good precision. The methodologies of this study may be applied in the future measurements made by the respective instruments.

Reference

1. B. Xu, W. C. Burnett, D. Lane-Smith, Z. Yu (2009). A simple laboratory-based radon calibration system. J Radioanal Nucl Chem. Pp. 1 – 8.
2. LaTour, M. S., & Tanner Jr, J. F. (2003). Radon: Appealing to our fears 1. Psychology & Marketing, 20(5), 377-394.
3. Rau, W., & Heusser, G. (2000). 222Rn emanation measurements at extremely low activities. Applied Radiation and Isotopes, 53(1-2), 371-375.
4. Wojcik, M., & Wlało, W. (1994). A high-sensitivity scintillation chamber for radon in gas. Nuclear Instruments and Methods in Physics Research Section A: Accelerators, Spectrometers, Detectors and Associated Equipment, 345(2), 351-355.
5. Wojcik, M., & Zuzel, G. (2008). A high-sensitivity large volume cryogenic detector for radon in gas. Journal of radioanalytical and nuclear chemistry, 277(1), 199-205.
6. Tokonami, S. (2020). Characteristics of thoron (220Rn) and its progeny in the indoor environment. International Journal of Environmental Research and Public Health, 17(23), 8769.
7. Kiko, J. (2001). Detector for 222Rn measurements in air at the 1 mBq/m3 level. Nuclear Instruments and Methods in Physics Research Section A: Accelerators, Spectrometers, Detectors and Associated Equipment, 460(2-3), 272-277.
8. Talha, S. A., De Meijer, R. J., Lindsay, R., Newman, R. T., Maleka, P. P., & Hlatshwayo, I. N. (2010). In-field radon measurement in water: a novel approach. Journal of environmental radioactivity, 101(12), 1024-1031.
9. Masevhe, L. (2017). An Analytical Study of Radon Concentration in Water from Some Rivers in Gauteng Using a Solid-State α− Detector (Doctoral dissertation, University of Johannesburg (South Africa)).
10. Zeeb, H., Shannoun, F., & World Health Organization. (2009). WHO handbook on indoor radon: a public health perspective. World Health Organization.
11. RAD-7, RAD H2O. Radon in Water Accessory, DuRRIDGE Co., user manual, pp. 31 – 48, 2012.
12. Hwang, D. W., Lee, I. S., Choi, M., & Kim, T. H. (2016). Estimating the input of submarine groundwater discharge (SGD) and SGD-derived nutrients in Geoje Bay, Korea using

222Rn-Si mass balance model. Marine Pollution Bulletin, 110(1), 119-126.
13. T. Yanliang and X. Detao. Revision for measuring the radon exhalation rate from the medium surface. IEEE Transactions on Nuclear Science. Vol, 58(1), 2011.
14. Alenezy, M. D. (2014). Radon concentrations measurement in Aljouf, Saudi Arabia using active detecting method. Natural Science, 2014.
15. Khattak, N., Khan, M., Shah, M., & Javed, M. (2011). Radon concentration in drinking water sources of the Main Campus of the University of Peshawar and surrounding areas, Khyber Pakhtunkhwa, Pakistan. Journal of Radioanalytical and Nuclear Chemistry, 290(2), 493-505.
16. K.Md. Najeeb and N. Vinaychandran. Radon contamination in groundwater and application of isotopes in groundwater studies. Journal of Geological Science, India, vol 77, pp 481 – 482, 2010.
17. S. Lorenz, T. Kaudse and W. Aeschbach-Hertig. F50/51 Limnophysics. Physics of Aquatic Systems, Institute of Environmental Physics in Heidelberg, Voslesungsskript, March, 2011.
18. Khan, H. A. (1991). Radon: a friend or a foe?. International Journal of Radiation Applications and Instrumentation. Part D. Nuclear Tracks and Radiation Measurements, 19(1-4), 353-362.
19. Schubert, M., Buerkin, W., Pena, P., Lopez, A. E., & Balcázar, M. (2006). On-site determination of the radon concentration in water samples: methodical background and results from laboratory studies and a field-scale test. Radiation measurements, 41(4), 492-497.
20. Xiaolin, H. (2009). Liquid scintillation counting for the determination of beta emitter principle and application. Riso National Laboratory for Sustainable Energy, Technical University of Denmark, NKS-B-Radwork shop-8.
21. Ellins, K. K., Roman-Mas, A., & Lee, R. (1990). Using 222Rn to examine groundwater/surface discharge interaction in the Rio Grande de Manati, Puerto Rico. Journal of Hydrology, 115(1-4), 319-341.
22. Kobayashi, Y. (1988). Laboratory manual for liquid scintillation counting. Packard Instrument.
23. Kessler, M. J. (1989). Liquid Scintillation Analysis–Science and Technology, Publication No. 169-3052 Packard Instrument Co. Inc., USA, 3-25.
24. Vajda, N., Martin, P., Kim, C. K., & L'Annunziata, M. F. (2012). Handbook of Radioactivity Analysis.
25. Csige, I., Szabó, Z., & Szabó, C. (2013). Experimental technique to measure thoron generation rate of building material samples using RAD7 detector. Radiation measurements, 59, 201-204.
26. Kim, G. (2011). Measurement and Application of Radium and Radon in the Environment.
27. Battat, J. B., Brack, J., Daw, E., Dorofeev, A., Ezeribe, A. C., Fox, J. R., ... & Yuriev, L. (2014). Radon in the DRIFT-II directional dark matter TPC: emanation, detection and mitigation. Journal of Instrumentation, 9(11), P11004.
28. Alenezy, M. D. (2014). Radon concentrations measurement in Aljouf, Saudi Arabia using active detecting method. Natural Science, 2014.